PERGAMON

International Journal of Solids and Structures 36 (1999) 4031–4049

INTERNATIONAL JOURNAL OF SOLIDS and STRUCTURES

Free vibration of axially loaded, rotating Timoshenko shaft systems by the wave-train closure principle

C. A. Tan*, B. Kang

Department of Mechanical Engineering, Wayne State University, Detroit, MI 48202, U.S.A.

Received 12 April 1998; in revised form 19 May 1998

Abstract

A systematic approach for the free vibration analysis of a rotating Timoshenko shaft system subjected to axial forces is presented in this paper. The system has multiple point discontinuities such as elastic supports, rotor masses, and cross-sectional changes. Wave reflection and transmission matrices are employed to characterize the wave motions between the sub-spans of the shaft system. These matrices are combined with the field transfer matrices expressed in wave forms to obtain the characteristic equation in a straightforward manner. The solutions are exact since effects of attenuating wave components are included in the formulation. The wave propagation-based matrix algebra leads to recursive algorithms which are suitable for computer coding. Three examples are presented to illustrate the numerical procedure.

Nomenclature

A_s	area of shaft cross-section [m^2]
a_0	diameter of shaft cross-section [m]
C, D	generalized coordinates of wave components
$\mathbf{C}$	incident or reflected wave vector
c_0	bar velocity [m/sec]
c_s	shear velocity [m/sec]
$\mathbf{D}$	transmitted wave vector
E, G	Young's and shear modulus [N/m^2], respectively
i	complex number, $\sqrt{-1}$
I	lateral moment of inertial of shaft [m^4]
J_M (J_m)	mass moment of inertial of a rotor mass [kg m^4]
K	Timoshenko shear coefficient

* Corresponding author. Fax: 001 313 577 8789; e-mail: tan@tan.eng.wayne.edu

0020–7683/99/$ - see front matter
PII: S0020–7683(98)00172–3

K_R (k_r) rotational spring (N-m/rad]
K_T (k_t) translational spring [N/m]
L_i (l_i) length of shaft [m], subscript i denotes span number
M (m) mass of rotor [kg]
P axial force [N]
R generalized reflection matrix
r_{ij}, t_{ij} reflection and transmission coefficients, respectively. $i = 1$ positive travelling wave; $i = 2$ negative travelling wave; Cases II and IV, $j = 1$ propagating wave, $j = 2$ attenuating wave. Case I, $j = 1, 2$ for propagating waves
T field transfer matrix
U (u) transverse displacement in the complex plane [m]
w wave vector
X-Y-Z(x-y-z) reference frame coordinates [m]

Greek symbols
α $(K \cdot G)/E$
β rotation parameter, see eqn (4)
ε $P/(E \cdot A)$, axial strain
$\hat{\varepsilon}$ non-dimensional axial load parameter, see eqn (11)
$\tilde{\Gamma}, \tilde{\gamma}$ (Γ, γ) wavenumber [m^{-1}]
ρ mass density of shaft [kg/m^3]
σ diameter ratio between two shaft elements
$\tilde{\omega}$, (ω) frequency [rad/s]
Ω rotation speed of shaft [rad/s]
ψ bending angle of the shaft cross-section [rad]
ξ local coordinate for wave reflection and transmission at discontinuities

Subscript
l, r the left and right side of a discontinuity, respectively

Superscript
$-$, $+$ negative and positive travelling waves, respectively, when used in C, D, and **w**. Otherwise denotes quantities on the left and right side of a discontinuity, respectively.
Note: Symbols in parenthesis are the corresponding non-dimensional parameters.

1. Introduction

Rotating flexible shafts are one of the most commonly employed mechanical elements for power transmission, high speed machining, and precision manufacturing. In each application, the reliability of the machinery depends on the stability of the rotating shaft elements and the use of accurate models for analysis especially for higher modes which are responsible for fatigue failure (Tsai and Wang, 1996). Three beam theories, the Euler–Bernouli, Rayleigh and Timoshenko models, are commonly used to describe the transverse vibrations of rotating flexible shafts. The Timoshenko model gives accurate predictions of the natural frequencies and vibration modes for

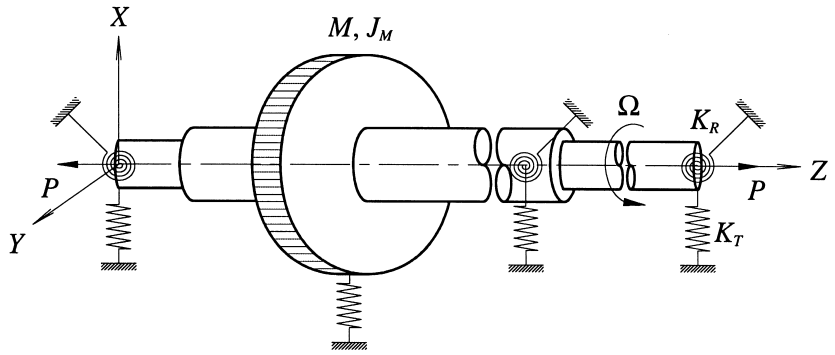

Fig. 1. Schematic of a rotating shaft system with multiple discontinuities and general boundary conditions.

stubby beams (Huang, 1961). In many modern applications of power transmission, for example, in automotive crankshaft mechanism, the rotating shaft span contains various discontinuities such as bearing supports, rotors, geometric changes in cross-sections, and non-classical boundary conditions (see Fig. 1). The general approach to the vibration problem is to consider the shaft as a system of multiple sub-spans and discontinuities. These spans usually have small slenderness ratios (length/diameter) and hence the Timoshenko beam theory should be used in the analysis.

The vibration of a rotating Timoshenko shaft has been studied by many and most papers are concerned with the development of solution techniques for evaluating the response and stability of different rotating shaft models (Zu and Han, 1992; Han and Zu, 1992; Katz et al., 1988; Lee et al., 1988). Tan and Kuang (1995) obtained exact, closed-form solutions for the free and forced responses of a stepped, rotating Timoshenko shaft by the distributed transfer function method and a generalized displacement formulation. The transfer function methodology was also applied to the analysis of non-uniform continuous systems by Yang and Fang (1994). Popplewell and Chang (1997) studied the stepped, spinning Timoshenko beam by the Galerkin method with polynomial based generalized force mode functions.

A commonly employed approach to study the vibrations of systems with multiple spans is the transfer matrix method which is well documented in the classical papers of Holzer (1921) and Myklestad (1944), and by Pestel and Leckie (1963). Due to its advantage of conciseness in the formulation that results from the use of matrix algebra, the transfer matrix method has been applied extensively to the analysis of complex structures and aircraft panels (Lin and Donaldson, 1969). Lee et al. (1991) examined the steady-state response of flexible rotor-bearing systems by representing the transfer matrix of the shaft as a continuous system.

The vibrations of elastic structures and the acoustics in fluids can be described in terms of waves propagating and attenuating in waveguides (Graff, 1975; Fahy, 1985). One advantage of using the wave propagation method to study the vibrations of structures is its ability to provide a compact and systematic methodology to analyze complex structures such as aircraft panels with periodic supports and beams on multiple supports (Yong, 1991). Employing the concept of wave reflection and transmission, Mace (1984) obtained the characteristic equations of Euler–Bernoulli beam models including both propagating and evanescent waves. By the phase closure principle (also called the wave-train closure principle (Cremer et al., 1973)), Mead (1994) calculated the natural

frequencies of Euler–Bernoulli beams. This principle states that if the phase difference between incident and reflected waves is an integer multiple of 2π, then the waves propagate at a natural frequency and their motions constitute a vibration mode. Despite the usefulness of the wave propagation technique, it has seldom been applied to study the vibration of rotating flexible shafts, except by Argento and Scott (1995) on an infinitely long rotating Timoshenko beam, and by Kang and Tan (1998), and Tan and Kang (1998) on the wave characteristic of an axially loaded shaft.

The equations of motion of an axially loaded, rotating Timoshenko shaft was derived by a finite strain theory (Choi et al., 1992). Employing the linearized equations of this model, Kang and Tan (1998) showed that the presence of the axial load and the rotation speed complicates the wave motions and in general there are three types of wave motions depending on the frequency and system parameters. Thus, for an axially loaded, rotating shaft with multiple discontinuities, there may be more than one type of wave motion in the elastic medium. It becomes difficult for many classical methods, such as the transfer matrix method, to be applied in a straightforward manner. For example, the field transfer matrix has different forms depending on whether the axial load is tension or compression (Subrahmanyam and Garg, 1997) and on the rotation speed. The transfer matrix method may also lead to computations of matrices of large orders if the structural system has different types of discontinuities (Yong, 1991). A systematic computation algorithm, capable of treating the combined effects of axial force, rotation speed and shear in a unified manner, is thus needed for the vibration analysis of rotating Timoshenko shaft systems.

The purpose of this paper is to present such an algorithm by combining the wave propagation technique and the compactness of the transfer matrix algebra. The method may be viewed as a matrix version of the wave-train closure principle. This paper is organized as follows. The vibration model and wave characteristics are summarized in Section 2. Wave reflection and transmission matrices and the wave-train closure principle are shown in Sections 3 and 4, respectively. Numerical examples are presented in Section 5, and conclusions are given in Section 6.

2. Problem formulation and harmonic wave solutions

Figure 1 shows a schematic of a shaft rotating about its longitudinal axis at a constant speed Ω and subject to axial load P. The shaft is elastically constrained at intermediate locations and the boundaries, and rigid rotor disks are mounted on it. For each sub-span, it is assumed that the material and geometric properties are uniform. Moreover, damping in the system is neglected, though the solution approach is still applicable for damped systems. The shaft model incudes the effects of rotary inertia, shear deformation, and axial deformation due to the axial load. Using a finite strain theory, the linearized equations governing the transverse and rotational motions (due to bending) of an infinitesimal element of the rotating shaft are given in the following non-dimensional form (Choi et al., 1992)

$$\frac{\partial^4 u}{\partial z^4} - (1+\alpha)\frac{\partial^4 u}{\partial z^2\,\partial t^2} + 2i\beta\frac{\partial^3 u}{\partial z^2\,\partial t} - 2i\beta\frac{\partial^3 u}{\partial t^3} + \alpha\frac{\partial^4 u}{\partial t^4} - 16\varepsilon\left(1+\varepsilon-\frac{\varepsilon}{\alpha}\right)\frac{\partial^2 u}{\partial z^2} + 16\alpha(1+\varepsilon)\left(1+\varepsilon-\frac{\varepsilon}{\alpha}\right)\frac{\partial^2 u}{\partial t^2} = 0, \quad (1)$$

$$\frac{\partial^4\psi}{\partial z^4}-(1+\alpha)\frac{\partial^4\psi}{\partial z^2\,\partial t^2}+2i\beta\frac{\partial^3\psi}{\partial z^2\,\partial t}-2i\beta\frac{\partial^3\psi}{\partial t^3}+\alpha\frac{\partial^4\psi}{\partial t^4}-16\varepsilon\left(1+\varepsilon-\frac{\varepsilon}{\alpha}\right)\frac{\partial^2\psi}{\partial z^2}$$
$$+16\alpha(1+\varepsilon)\left(1+\varepsilon-\frac{\varepsilon}{\alpha}\right)\frac{\partial^2\psi}{\partial t^2}=0, \quad (2)$$

where the complex displacement u and rotation ψ satisfy the kinematic relationship

$$\frac{\partial^2 u}{\partial t^2}=\frac{\partial^2 u}{\partial z^2}+i\left(1+\varepsilon-\frac{\varepsilon}{\alpha}\right)\frac{\partial\psi}{\partial z}, \quad (3)$$

and the following non-dimensional variables and parameters have been introduced.

$$u=\frac{U}{a_0},\quad z=\frac{Z}{a_0},\quad t=\frac{T}{T_0},\quad T_0=\sqrt{\frac{\rho a_0^2}{KG}};\quad \alpha=\frac{KG}{E},\quad \beta=\frac{\rho a_0^2}{ET_0}\Omega,\quad \varepsilon=\frac{P}{EA_s}. \quad (4)$$

A list of notations is given in the Nomenclature.

Development of the wave solutions for the shaft model has been discussed in a previous work (Kang and Tan, 1998). Here, only equations relevant to the current study are presented. Assume harmonic wave solutions to eqns (1) and (2) as

$$u(z,t)=C_u\,e^{i(\gamma z+\omega t)},\quad \psi(z,t)=C_\psi\,e^{i(\gamma z+\omega t)}, \quad (5a,b)$$

where γ and ω are non-dimensional wavenumber and frequency defined as

$$\gamma=\tilde{\gamma}a_0,\quad \omega=\frac{\tilde{\omega}a_0}{c_s}\left(c_s=\sqrt{\frac{KG}{\rho}}\text{ is the shear velocity}\right). \quad (6)$$

Substituting the wave solution (5a) into eqn (1) leads to the frequency equation

$$\alpha\omega^4-2\beta\omega^3-[(1+a)\gamma^2+16\alpha(1+\varepsilon)\hat{\varepsilon}]\omega^2+2\beta\gamma^2\omega+\gamma^2[\gamma^2+16\varepsilon\hat{\varepsilon}]=0, \quad (7)$$

or in terms of wavenumber γ,

$$\gamma^4-A\gamma^2+B=0, \quad (8)$$

where,

$$A=(1+\alpha)\omega^2-2\beta\omega-16\varepsilon\hat{\varepsilon}, \quad (9)$$

$$B=\omega^2[\alpha\omega^2-2\beta\omega-16\alpha(1+\varepsilon)\hat{\varepsilon}], \quad (10)$$

$$\hat{\varepsilon}=1+\varepsilon-\frac{\varepsilon}{\alpha}. \quad (11)$$

The four roots of eqn (8) are

$$\gamma=\pm\frac{1}{\sqrt{2}}(A\pm\sqrt{A^2-4B})^{1/2}. \quad (12)$$

For $\alpha > 0$ and $|\varepsilon| < 1$, it can be shown that the discriminant A^2-4B is semi-positive definite for most engineering applications. Employing this fact and assuming that ω is real, it is readily shown that γ is either real or imaginary. The general wave solutions can then be classified into four cases as follows.

Case I ($A > 0$ and $B > 0$; all roots of eqn (8) are real)

$$u(z,t) = (C_1^+ \, e^{-i\gamma_1 z} + C_1^- \, e^{i\gamma_1 z} + C_2^+ \, e^{-i\gamma_2 z} + C_2^- \, e^{i\gamma_2 z}) \, e^{i\omega t}, \tag{13a}$$

$$\psi(z,t) = (\eta_1 C_1^+ \, e^{-i\gamma_1 z} - \eta_1 C_1^- \, e^{i\gamma_1 z} + \eta_2 C_2^+ \, e^{-i\gamma_2 z} - \eta_2 C_2^- \, e^{i\gamma_2 z}) \, e^{i\omega t}, \tag{13b}$$

where, by eqn (3), η_1 and η_2 are

$$\eta_1 = \frac{\gamma_1^2-\omega^2}{\gamma_1 \hat{\varepsilon}}, \quad \eta_2 = \frac{\gamma_2^2-\omega^2}{\gamma_2 \hat{\varepsilon}}. \tag{13c}$$

Case II ($A > 0$ and $B < 0$; two roots of eqn (8) are real and two are imaginary)

$$u(z) = (C_1^+ \, e^{-i\Gamma_1 z} + C_1^- \, e^{i\Gamma_1 z} + C_2^+ \, e^{-\Gamma_2 z} + C_2^- \, e^{\Gamma_2 z}) \, e^{i\omega t}, \tag{14a}$$

$$\psi(z) = (\eta_1 C_1^+ e^{-i\Gamma_1 z} - \eta_1 C_1^- \, e^{i\Gamma_1 z} + \eta_2 C_2^+ \, e^{-\Gamma_2 z} - \eta_2 \, C_2^- e^{\Gamma_2 z}) \, e^{i\omega t}, \tag{14b}$$

where,

$$\eta_1 = \frac{\Gamma_1^2-\omega^2}{\Gamma_1 \hat{\varepsilon}}, \quad \eta_2 = \frac{\Gamma_2^2+\omega^2}{i\Gamma_2 \hat{\varepsilon}}. \tag{14c}$$

Case III ($A < 0$ and $B > 0$; all roots of eqn (8) are imaginary)

$$u(z,t) = C_1^+ \, e^{-\gamma_1 z} + C_1^- \, e^{\gamma_1 z} + C_2^+ \, e^{-\gamma_2 z} + C_2^- \, e^{\gamma_2 z}) \, e^{i\omega t}, \tag{15a}$$

$$\psi(z,t) = \eta_1 C_1^+ \, e^{-\gamma_1 z} - \eta_1 C_1^- \, e^{\gamma_1 z} + \eta_2 C_2^+ \, e^{-\gamma_2 z} - \eta_2 C_2^- \, e^{\gamma_2 z}) \, e^{i\omega t} \tag{15b}$$

where,

$$\eta_1 = \frac{\gamma_1^2+\omega^2}{i\gamma_1 \hat{\varepsilon}}, \quad \eta_2 = \frac{\gamma_2^2+\omega^2}{i\gamma_2 \hat{\varepsilon}}. \tag{15c}$$

Case IV ($A < 0$ and $B < 0$; two roots of eqn (8) are real and two are imaginary)

$$u(z,t) = (C_1^+ \, e^{-\Gamma_1 z} + C_1^- \, e^{\Gamma_1 z} + C_2^+ \, e^{-i\Gamma_2 z} + C_2^- \, e^{i\Gamma_2 z}) \, e^{i\omega t}, \tag{16a}$$

$$\psi(z,t) = (\eta_1 C_1^+ \, e^{-\Gamma_1 z} - \eta_1 C_1^- \, e^{\Gamma_1 z} + \eta_2 C_2^+ \, e^{-i\Gamma_2 z} - \eta_2 C_2^- \, e^{i\Gamma_2 z}) \, e^{i\omega t}, \tag{16b}$$

where,

$$\eta_1 = \frac{\Gamma_1^2+\omega^2}{i\Gamma_1 \hat{\varepsilon}}, \quad \eta_2 = \frac{\Gamma_2^2-\omega^2}{\Gamma_2 \hat{\varepsilon}}. \tag{16c}$$

In above equations, the following wavenumbers have been defined

$$\gamma_1 = \frac{1}{\sqrt{2}}(|A| + \sqrt{A^2-4|B|})^{1/2}, \quad \gamma_2 = \frac{1}{\sqrt{2}}(|A| - \sqrt{A^2-4|B|})^{1/2}, \tag{17a}$$

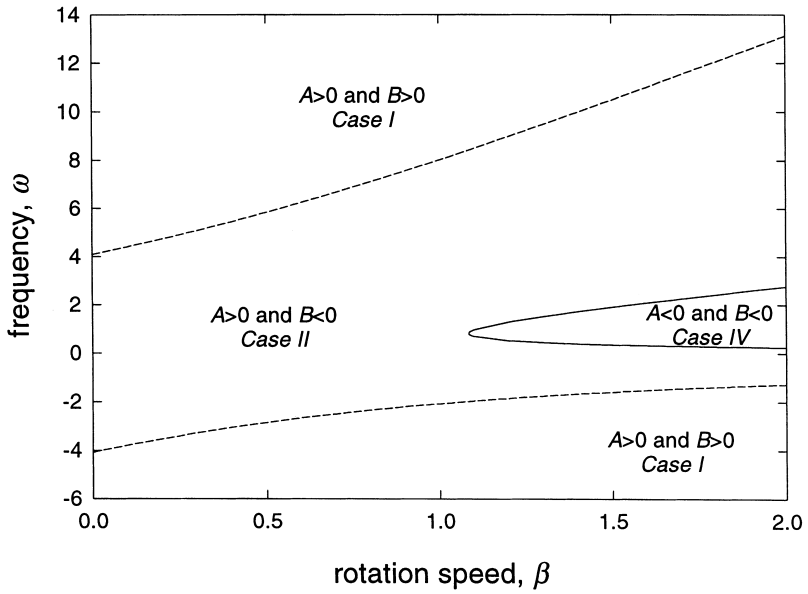

Fig. 2. Frequency spaces demarcated by the non-zero cutoff frequencies ($B = 0$) and $A = 0$, as a function of β with $\varepsilon = -0.05$ (compression); $A =$ (—), $B = 0$ (- - -).

$$\Gamma_1 = \frac{1}{\sqrt{2}}(\sqrt{A^2+4|B|}+|A|)^{1/2}, \quad \Gamma_2 = \frac{1}{\sqrt{2}}(\sqrt{A^2+4|B|}-|A|)^{1/2}. \tag{17b}$$

Note that the coefficients C_i^+ and C_i^- denote the transverse amplitudes of positive-traveling and negative-traveling waves from the origin of disturbance along the shaft, respectively. Among these four wave solutions, the solution of Case III does not exist in the real frequency space since none of the wave components can propagate along the shaft, as seen in eqns (15a,b). Therefore, this type of wave solution is of no interest in vibration problems. Note that, for the Timoshenko model, there exists a non-zero cutoff frequency above which all wave components propagate. In this frequency range, the motion is governed by the solution of Cases I. Below the cutoff frequency, two wave components propagate and the wave motions are governed by the solution of Case II or IV depending on the system parameters. Figure 2 shows the frequency spaces demarcated by the non-zero cutoff frequencies ($B = 0$) and $A = 0$, as a function of the rotation speed with $\varepsilon = -0.05$ (compression). In each region, one of the three wave solutions applies. It is important to note that, for this amount of compression and at sufficiently large β, the form of the wave solution changes from Case IV to Case II. This kind of transition depends strongly on the axial load. In summary, because of the multiple wave solutions, one must note that different vibration modes may be associated with different types of wave solutions.

3. Wave reflection and transmission matrices

When a wave is incident upon a discontinuity such as an intermediate support, a different waveguide, or a boundary, it is reflected and/or transmitted depending on the properties of the

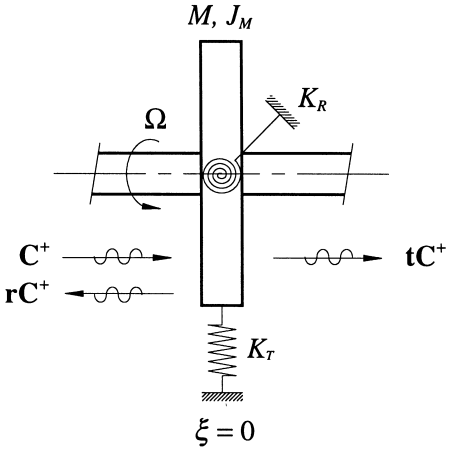

Fig. 3. Wave reflection and transmission at a kinetic discontinuity.

discontinuity. In general, a wave component either propagates or attenuates (evanescent or near-field). However, for a Timoshenko model, there exists a finite cutoff frequency above which all wave components propagate due to the effects of the shear deformations. When the distances between discontinuities are relatively small, attenuating components play an important role in the wave motions by contributing significant amounts of energy to the total power flow (Graff, 1975). In this section, wave reflection and transmission matrices for the rotating shaft model are obtained for various kinds of discontinuities. These matrices are needed for the wave-train closure principle.

3.1. Wave reflection and transmission at a kinetic discontinuity

Consider a rotating Timoshenko shaft element supported at a local coordinate $\xi = 0$; see Fig. 3. The support consists of linear transverse and rotational springs, and a rigid rotor mass which typically represents a gear transmitting a torque. By eqns (13)–(16), group the wave components into 2×1 vectors of positive-traveling waves $\mathbf{C}^+$ and negative-traveling waves $\mathbf{C}^-$,

$$\mathbf{C}^+ = \begin{Bmatrix} C_1^+ \\ C_2^+ \end{Bmatrix}, \quad \mathbf{C}^- = \begin{Bmatrix} C_1^- \\ C_2^- \end{Bmatrix}. \tag{18a,b}$$

When a set of positive-traveling waves $\mathbf{C}^+$ is incident upon the support, it gives rise to a set of reflected waves $\mathbf{C}^-$ and transmitted waves $\mathbf{D}^+$. These waves are related by

$$\mathbf{C}^- = \mathbf{r}\mathbf{C}^+, \quad \mathbf{D}^+ = \mathbf{t}\mathbf{C}^+ \tag{19a,b}$$

where $\mathbf{r}$ and $\mathbf{t}$ are the 2×2 reflection and transmission matrices, respectively.

Applying the displacement continuity and force and moment balance at the support, $\mathbf{r}$ and $\mathbf{t}$ can be obtained. Note that since there are four (practically three) different wave motions in our rotating Timoshenko shaft model, a different set of $\mathbf{r}$ and $\mathbf{t}$ for each Case needs to be derived. In this paper, only the expressions of $\mathbf{r}$ and $\mathbf{t}$ for Case II are presented. Similar procedures can be applied to derive the reflection and transmission matrices for other cases. It should be noted that Cases II

and IV govern the wave motions in the vibration frequency ranges encountered in most engineering problems. Introduce the following non-dimensional parameters

$$k_t = \frac{K_t a_0}{KAG}, \quad k_r = \frac{K_r a_0}{EI}, \quad m = \frac{M}{\rho A a_0}, \quad \text{and} \quad J_m = \frac{J_M c_s^2}{EI}. \tag{20}$$

Denote $\mathbf{r}_{II}$ and $\mathbf{t}_{II}$ as the reflection and transmission matrices for Case II of the wave incident upon the support depicted in Fig. 3, respectively,

$$\mathbf{r}_{II} = \frac{1}{\Delta}\begin{bmatrix} r_{11} & r_{12} \\ r_{21} & r_{22} \end{bmatrix}, \quad \mathbf{t}_{II} = \frac{1}{\Delta}\begin{bmatrix} t_{11} & t_{12} \\ t_{21} & t_{22} \end{bmatrix}. \tag{21a,b}$$

The elements of $\mathbf{r}_{II}$ and $\mathbf{t}_{II}$ can be derived as

$$\begin{aligned}
\Delta &= \{\eta_1(2\Gamma_1 - iH_m) + i\eta_2(2\Gamma_1 + H_m)\}\{2\eta_1\Gamma_2 - 2i\eta_2\Gamma_1 + H_s(\eta_1 - \eta_2)\}, \\
r_{11} &= -2\eta_1\eta_2\Gamma_1(H_m - H_s) + i\eta_2^2 H_s(2\Gamma_2 + H_m) - i\eta_1^2 H_m(2\Gamma_2 + H_s), \\
r_{12} &= -2\eta_2[i\eta_1\{\Gamma_2 H_m + H_s(i\Gamma_1 + H_m)\} + \eta_2\{\Gamma_1 H_m - iH_s(\Gamma_2 + H_m)\}], \\
r_{21} &= 2\eta_1[i\eta_1\{\Gamma_2 H_m + H_s(i\Gamma_1 + H_m)\} + \eta_2\{\Gamma_1 H_m - iH_s(\Gamma_2 + H_m)\}], \\
r_{22} &= 2i\eta_1\eta_2\Gamma_2(H_m - H_s) + \eta_2^2 H_m(2\Gamma_1 - iH_s) + \eta_1^2 H_s(iH_m - 2\Gamma_1), \\
t_{11} &= 2\eta_2^2\Gamma_1(2\Gamma_2 + H_m) + 2\eta_1^2\Gamma_1(2\Gamma_2 + H_s) - 2i\eta_1\eta_2\{2\Gamma_1^2 - \Gamma_2(2\Gamma_2 + H_m + H_s)\}, \\
t_{12} &= 2\eta_2(\eta_2\Gamma_1 H_m + i\eta_1\Gamma_2 H_m + \eta_1\Gamma_1 H_s + i\eta_2\Gamma_2 H_s), \\
t_{21} &= -2\eta_1(\eta_2\Gamma_1 H_m + i\eta_1\Gamma_2 H_m + \eta_1\Gamma_1 H_s + i\eta_2\Gamma_2 H_s), \\
t_{22} &= 2\eta_1^2\Gamma_2(2\Gamma_1 - iH_m) + 2\eta_2^2\Gamma_2(2\Gamma_1 - iH_s) + 2\eta_1\eta_2\{2i\Gamma_2^2 - 2i\Gamma_1^2 - \Gamma_1(H_m + H_s)\}, \\
H_m &= k_r - J_m\omega^2, \quad H_s = k_t - m\omega^2.
\end{aligned} \tag{22}$$

$\mathbf{r}_{IV}$ and $\mathbf{t}_{IV}$ for Case IV can be obtained by replacing $i\Gamma_1$ and Γ_2 in the above expressions with Γ_1 and $i\Gamma_2$, respectively.

3.2. Wave reflection and transmission at a cross-sectional change

When a wave travels across a discontinuity due to a change in the cross-section or material properties, its wavelength is changed. Consider the shaft model with two elements of different diameters joined at $\xi = 0$ as shown in Fig. 4. For simplicity, assume that the material properties ρ, E and G of both shaft elements are the same. The derivation procedure is the same even if the material properties are different. Denote the subscripts l and r as $\xi = 0^-$ and $\xi = 0^+$, respectively. The wavenumbers, A and B at the right side of the discontinuity are

$$\gamma_{1r} = \frac{1}{\sqrt{2}}(A_r + \sqrt{A_r^2 - 4B_r})^{1/2}, \quad \gamma_{2r} = \frac{1}{\sqrt{2}}(A_r - \sqrt{A_r^2 - 4B_r})^{1/2}, \tag{23a}$$

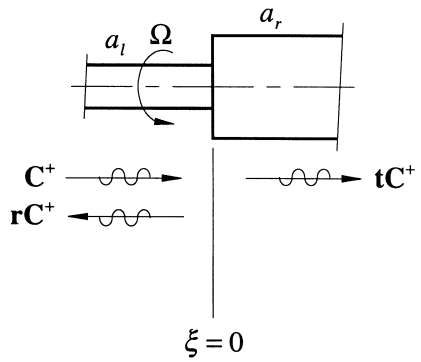

Fig. 4. Wave reflection and transmission at a cross-sectional change.

$$\Gamma_{1r} = \frac{1}{\sqrt{2}}(\sqrt{A_r^2 + 4|B_r|} + |A_r^2|)^{1/2}, \quad \Gamma_{2r} = \frac{1}{\sqrt{2}}(\sqrt{A_r^2 + 4|B_r|} - |A_r^2|)^{1/2}, \tag{23b}$$

where

$$A_r = (1+\alpha)\omega^2 - 2\beta\omega - \frac{16}{\sigma^2}\varepsilon_r\hat{\varepsilon}_r, \tag{24}$$

$$B_r = \omega^2\left[\alpha\omega^2 - 2\beta\omega - \frac{16}{\sigma^2}\alpha(1+\varepsilon_r)\hat{\varepsilon}_r\right], \tag{25}$$

$$\hat{\varepsilon}_r = 1 + \varepsilon_r - \frac{\varepsilon_r}{\alpha}, \quad \varepsilon_r = \frac{\varepsilon}{\sigma^2}, \quad \sigma = \frac{a_r}{a_l} \quad \text{(diameter ratio)}. \tag{26}$$

Corresponding quantities at the left side of the discontinuity have the same expressions but with $\sigma = 1$.

It is possible that a wave propagating in $\xi = 0^-$ becomes attenuating after crossing the discontinuity. The wave motions on both sides of the discontinuity can be different depending on the frequencies and system parameters. Therefore, for a rotating Timoshenko shaft, there are mathematically nine possible combinations of wave motions to be considered since each side of the discontinuity has three wave motions, Cases I, II, and IV depending on the values of A and B. To illustrate the formulation of the wave reflection and transmission matrices, suppose the wave motions on the left and right sides of the discontinuity are of Case II and Case I, respectively. Then, imposing the displacement continuity and force and moment balance at the discontinuity leads to the following matrix equations.

$$\begin{bmatrix} 1 & 1 \\ \eta_{1l} & \eta_{2l} \end{bmatrix}\mathbf{C}^+ + \begin{bmatrix} 1 & 1 \\ -\eta_{1l} & \eta_{2l} \end{bmatrix}\mathbf{r}_{II-I}\mathbf{C}^+ = \begin{bmatrix} 1 & 1 \\ \eta_{1r} & \eta_{2r} \end{bmatrix}\mathbf{t}_{II-I}\mathbf{C}^+, \tag{27a}$$

$$\begin{bmatrix} i\Gamma_{1l}\eta_{1l} & -\Gamma_{2l}\eta_{2l} \\ i(\eta_{1l}-\Gamma_{1l}) & i\eta_{2l}-\Gamma_{2l} \end{bmatrix}\mathbf{C}^{+}+\begin{bmatrix} -i\Gamma_{1l}\eta_{1l} & -\Gamma_{2l}\eta_{2l} \\ i(\Gamma_{1l}-\eta_{1l}) & (\Gamma_{2l}-i\eta_{2l}) \end{bmatrix}\mathbf{r}_{\mathrm{II-I}}\mathbf{C}^{+}$$

$$=\begin{bmatrix} -i\sigma^{4}\gamma_{1r}\eta_{1r} & -i\sigma^{4}\gamma_{2r}\eta_{2r} \\ i\sigma^{2}(\eta_{1r}-\gamma_{1r}) & i\sigma^{2}(\eta_{2r}-\gamma_{2r}) \end{bmatrix}\mathbf{t}_{\mathrm{II-I}}\mathbf{C}^{+}, \quad (27b)$$

where, the subscripts II–I of **r** and **t** denote a transition of the wave solutions in that order. Note that η_{il} in eqns (27a,b) are given by eqn (14c) and η_{ir} for each Case are

$$\eta_{1r}=\frac{\gamma_{1r}^{2}-\omega^{2}}{\gamma_{1r}\hat{\varepsilon}_{r}}, \quad \eta_{2r}=\frac{\gamma_{2r}^{2}-\omega^{2}}{\gamma_{2r}\hat{\varepsilon}_{r}} \quad \text{for Case I,} \quad (28)$$

$$\eta_{1r}=\frac{\Gamma_{1r}^{2}-\omega^{2}}{\Gamma_{1r}\hat{\varepsilon}_{r}}, \quad \eta_{2r}=\frac{\Gamma_{2r}^{2}+\omega^{2}}{i\Gamma_{2r}\hat{\varepsilon}_{r}} \quad \text{for Case II,} \quad (29)$$

$$\eta_{1r}=\frac{\Gamma_{1r}^{2}+\omega^{2}}{i\Gamma_{1r}\hat{\varepsilon}_{r}}, \quad \eta_{2r}=\frac{\Gamma_{2r}^{2}-\omega^{2}}{\Gamma_{2r}\hat{\varepsilon}_{r}} \quad \text{for Case IV} \quad (30)$$

where γ_{ir} and Γ_{ir} are given by eqns (23a,b). The explicit expressions for $\mathbf{r}_{\mathrm{II-I}}$ and $\mathbf{t}_{\mathrm{II-I}}$ are not presented in this paper due to space limitation. However, they can be obtained from the solutions of eqns (27a,b) in either closed-form or numerically. The reflection and transmission matrices for other cases such as $\mathbf{r}_{\mathrm{I-II}}$, $\mathbf{t}_{\mathrm{I-II}}$, $\mathbf{r}_{\mathrm{IV-II}}$, and $\mathbf{t}_{\mathrm{IV-II}}$ can be obtained in a similar manner.

3.3. Wave refection at a boundary

When a wave is incident at a boundary, it is only reflected. Consider an arbitrary boundary conditions with translational and rotational springs, and a rigid rotor mass (for a right boundary, see Fig. 3 without the shaft element on the right side). By imposing the force and moment balance at the boundary, the reflection matrix at the boundary can be derived for each Case. For example, $\mathbf{r}_{\mathrm{II}}$ can be expressed as

$$\mathbf{r}_{\mathrm{II}}=\begin{bmatrix} \eta_{1}(i\Gamma_{1}+H_{\mathrm{m}}) & \eta_{2}(\Gamma_{2}+H_{\mathrm{m}}) \\ i(\Gamma_{1}-\eta_{1})+H_{\mathrm{s}} & (\Gamma_{2}-i\eta_{2})+H_{\mathrm{s}} \end{bmatrix}^{-1}\begin{bmatrix} -\eta_{1}(i\Gamma_{1}-H_{\mathrm{m}}) & -\eta_{2}(\Gamma_{2}-H_{\mathrm{m}}) \\ i(\Gamma_{1}-\eta_{1})-H_{\mathrm{s}} & (\Gamma_{2}-i\eta_{2})-H_{\mathrm{s}} \end{bmatrix}, \quad (31)$$

where, H_{m} and H_{s} are given by eqn (22). Note that $\mathbf{r}_{\mathrm{IV}}$ can be obtained by replacing $i\Gamma_{1}$ and Γ_{2} in the above expression with Γ_{1} and $i\Gamma_{2}$, respectively. $\mathbf{r}_{\mathrm{I}}$ can be obtained in a similar manner by applying the wave solution of Case I.

4. Free vibration analysis

The reflection and transmission matrices of waves incident upon point discontinuities can be combined with the transfer matrix method to analyze the free vibration of the rotating shaft system shown in Fig. 1. The basic idea of this technique is known as the wave-train or phase closure principle which has been presented for non-rotating Euler–Bernoulli beams (Mead, 1994; Mace, 1984; Cremer et al., 1973). However, due to the complexity of wave motions in the Timoshenko

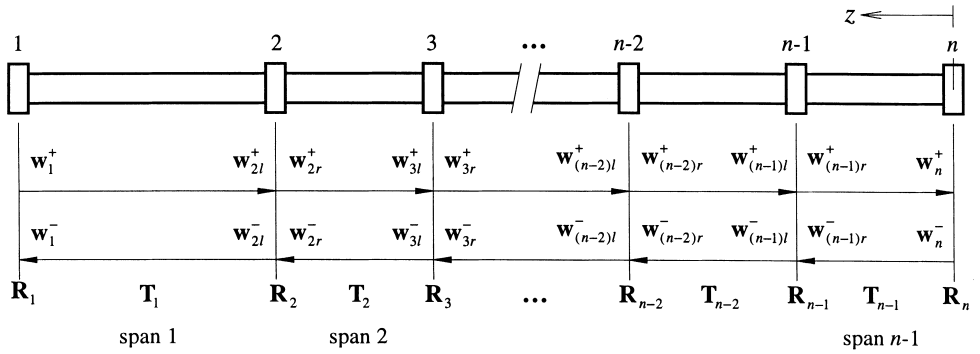

Fig. 5. A rotating shaft model with multi-discontinuities and general boundary conditions.

shaft model (such as multiple wave solutions and the frequency dependence of the wave reflection and transmission at a cross-sectional change), it is important to apply the proper wave reflection and transmission matrices consistent with the values of A and B on both sides of the discontinuity. In this section, we apply the wave-train closure principle to the rotating Timoshenko shaft system.

Consider a rotating Timoshenko shaft with n discontinuities and general boundaries as shown in Fig. 5. Define $\mathbf{R}_i$ as a generalized reflection matrix which relates the amplitudes of negative and positive traveling waves at station (discontinuity) i and $\mathbf{T}_i$ as the field transfer matrix between stations i and $i+1$ which relates the wave amplitudes by

$$\mathbf{w}^+(z_0+z) = \mathbf{T}\mathbf{w}^+(z_0) \quad \text{or } \mathbf{w}^-(z_0+z) = \mathbf{T}^{-1}\mathbf{w}^-(z_0), \tag{32}$$

where,

$$\mathbf{T} = \begin{bmatrix} e^{-i\gamma_1 z} & 0 \\ 0 & e^{-i\gamma_2 z} \end{bmatrix} \quad \text{for Case I,} \tag{33}$$

$$\mathbf{T} = \begin{bmatrix} e^{-i\Gamma_1 z} & 0 \\ 0 & e^{-\Gamma_2 z} \end{bmatrix} \quad \text{for Case II,} \tag{34}$$

$$\mathbf{T} = \begin{bmatrix} e^{-\Gamma_1 z} & 0 \\ 0 & e^{-i\Gamma_2 z} \end{bmatrix} \quad \text{for Case IV} \tag{35}$$

By these definitions, the following relations can be obtained

$$\mathbf{w}_n^- = \mathbf{R}_n \mathbf{w}_n^+, \quad (\mathbf{R}_n = \mathbf{r}_n), \tag{36}$$

$$\mathbf{w}_{ij}^- = \mathbf{R}_{ij}\mathbf{w}_{ij}^+, \quad \begin{cases} i = 2,3,\ldots,n-1 \quad \text{(station number)} \\ j = \text{l (left) or r (right)}, \end{cases} \tag{37}$$

$$\mathbf{w}_1^- = \mathbf{T}_1 w_{2l}^-, \tag{38}$$

$$\mathbf{w}_1^+ = \mathbf{R}_1 \mathbf{w}_1^- \quad (\mathbf{R}_1 = \mathbf{r}_1), \tag{39}$$

$$\mathbf{w}_{2l}^{+} = \mathbf{T}_1 \mathbf{w}_1^{+}, \tag{40}$$

where, in eqn (37),

$$\mathbf{R}_{il} = \mathbf{r}_i + \mathbf{t}_i(\mathbf{R}_{ir}^{-1} - \mathbf{r}_i)^{-1}\mathbf{t}_i, \quad \mathbf{R}_{ir} = \mathbf{T}_i \mathbf{R}_{(i+1)l} \mathbf{T}_i. \tag{41a,b}$$

Attention should be paid in formulating $\mathbf{R}_{il}$ when waves travel across a cross-sectional change. Suppose the wave motions in span 1 and span 2 in Fig. 5 are governed by Case I and Case II, respectively. Then, the incoming and outgoing waves at station 2 are related by

$$\mathbf{w}_{2r}^{+} = \mathbf{t}_{I-II}\mathbf{w}_{2l}^{+} + \mathbf{r}_{II-I}\mathbf{w}_{2r}^{-}, \tag{42a}$$

$$\mathbf{w}_{2l}^{-} = \mathbf{t}_{II-I}\mathbf{w}_{2r}^{-} + \mathbf{r}_{I-II}\mathbf{w}_{2l}^{+}. \tag{42b}$$

Since $\mathbf{w}_{2r}^{-} = \mathbf{R}_{2r}\mathbf{w}_{2r}^{+}$, eqns (42a, b) can be combined to give

$$\mathbf{w}_{2l}^{-} = \mathbf{R}_{2l}\mathbf{w}_{2l}^{+}, \quad \text{where } \mathbf{R}_{2l} = \mathbf{r}_{I-II} + \mathbf{t}_{II-I}(\mathbf{R}_{2l}^{-1} - \mathbf{r}_{II-I})^{-1}\mathbf{t}_{I-II}. \tag{43}$$

Therefore, for a geometric discontinuity, two sets of reflection and transmission matrices are needed to formulate $\mathbf{R}$. Note that, for geometrically uniform spans, eqn (43) reduces to eqn (41a). Solving the above matrix eqns (36)–(40) gives

$$(\mathbf{R}_1\mathbf{T}_1\mathbf{R}_{2l}\mathbf{T}_1 - \mathbf{I})\mathbf{w}_1^{+} = 0. \tag{44}$$

For non-trivial solutions, the natural frequencies are obtained form the characteristic equation

$$C(\omega) = \mathrm{Det}\,[(\mathbf{R}_1\mathbf{T}_1\mathbf{R}_{2l}\mathbf{T}_1 - \mathbf{I})] = 0. \tag{45}$$

When the shaft is geometrically uniform and has homogeneous material properties in all the spans, the wave motions is governed by a single solution form at a given frequency. In this case, since the values of A and B are identical for the spans, formulation of $C(\omega)$ is straightforward. However, in general, one needs to consider two or three different wave solutions in the spans, depending on the frequencies and the properties of the discontinuities. Hence, in the derivation of $C(\omega)$, the reflection and transmission matrices at each station and the field transfer matrix for each span must be properly determined.

5. Numerical examples

Three numerical examples are presented to demonstrate the applications of the wave-train closure principle. The first example is a non-rotating shaft (one meter long) supported by elastic springs at $z = 0$, 0.4 , 1 m. A schematic of the system is shown on the top of Fig. 6. The non-dimensional lengths of the two sub-spans are $l_1 = 0.4/a_0$ and $l_2 = 0.6/a_0$ with $a_0 = 0.0955$ m. The spring stiffness constants are $k_t = 0.1907$ and $k_r = 113$. Figure 6 plots $C(\omega)$ as a function of frequency, and compares results from the present wave approach with those obtained by the standard method of separation of variables. It should be noted that the wave approach always results in evaluating the determinant of a 2×2 matrix [see eqn (45)]. However, a matrix of size $4n \times 4n$ ($n = 2$ in this example) needs to be considered in the separation of variables method.

As shown in Fig. 6, the separation of variables method gives a $C(\omega)$ which has very large slopes near the natural frequencies. This makes the search for the roots of $C(\omega)$ extremely difficult since

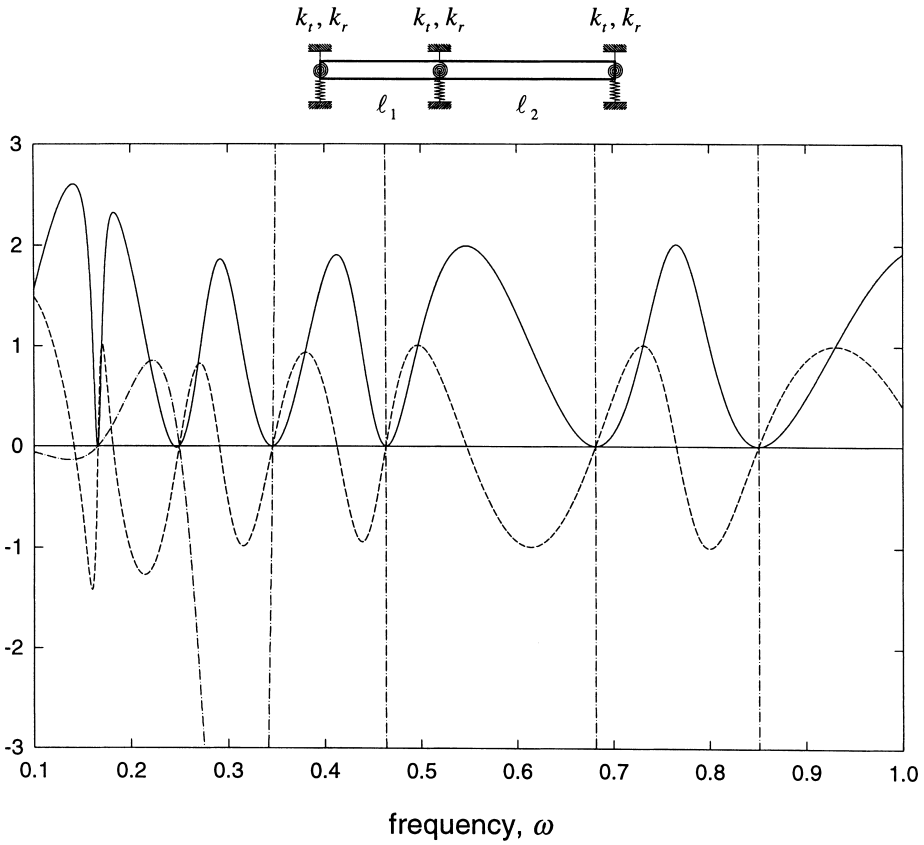

Fig. 6. Plot of $C(\omega)$ as a function of frequency, $\alpha = 0.3378$, $\beta = 0$, $\varepsilon = 0$, $k_t = 0.1907$, $k_r = 113$, $l_1 = 0.4/a_0$, $l_2 = 0.6/a_0$, $a_0 = 0.0955$ m; Re $[C(\omega)]$ (—), Im $[C(\omega)]$ (- - -). Dot–dashed curve (–·–) shows the result obtained from the standard method of separation of variables.

the convergence of most root-finding routines (e.g., secant method) depends strongly on the slopes of the curve near the roots. Moreover, though not shown, the amplitude of oscillation of $C(\omega)$ increases exponentially with ω in the separation of variables method. It should be noted that, although both methods lead to the same roots, the wave approach produces a different characteristic equation from which the natural frequencies can be searched more easily. Mead (1994) also showed that the phase closure principle led to a different characteristic equation for the Euler–Bernoulli beam. As pointed out by Mace (1984), the only source of numerical difficulty in this wave approach occurs when flexural components of the whole system contain an insignificant amount of the total mass or flexibility of the system. The beam spans then appear physically as rigid bodies or massless elements. The wavenumber becomes small and the representation of the beam displacement in terms of waves becomes unrealistic. This situation leads to significant rounding errors in the computations. In practice, however, the contribution of beam mass and flexibility, although small, is enough to overcome these difficulties.

The second example is a rotating shaft with an intermediate elastic support and a rotor mass,

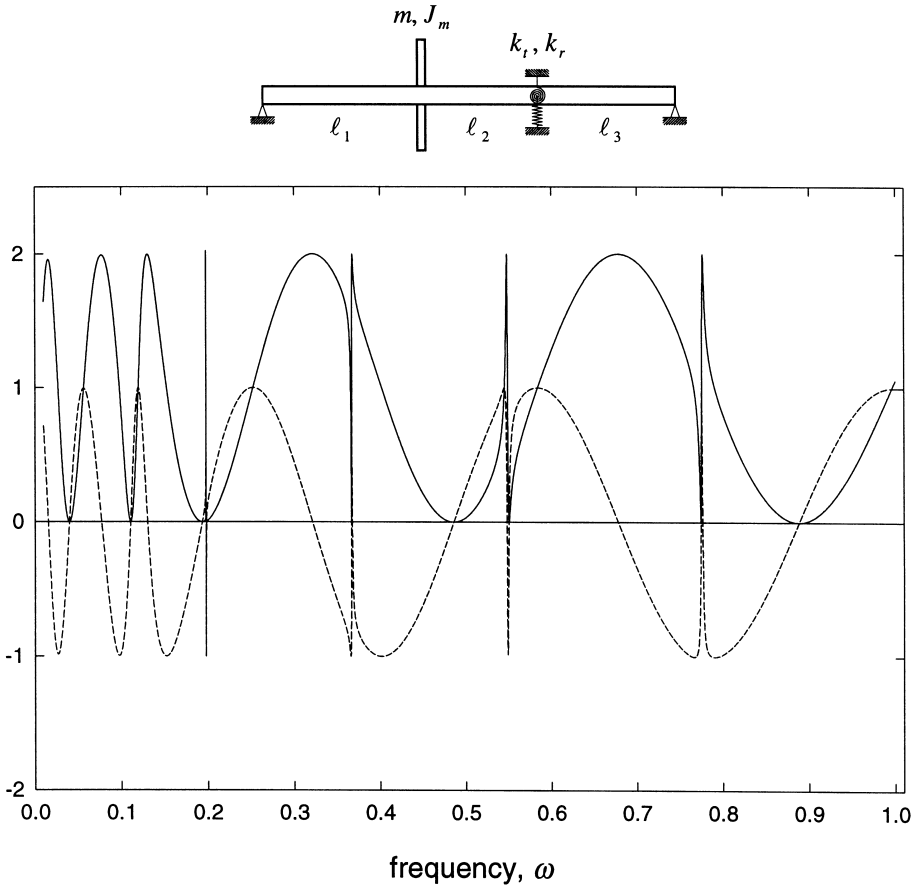

Fig. 7. Plot of $C(\omega)$ as a function of frequency, $\alpha = 0.3378$, $\beta = 0.05$, $\varepsilon = -0.002$, $k_t = 0.3814$, $k_r = 113$, m = 4.7120, $J_m = 86$, $l_1 = 06/a_0$, $l_2 = 0.4/a_0$, $l_3 = 0.5/a_0$, $a_0 = 0.0955$ m; Re $[C(\omega)]$ (—), Im $[C(\omega)]$ (- - -).

and a compressive axial load is applied. A schematic of the system is depicted on the top of Fig. 7. The total length of the shaft is 1.5 m and the non-dimensional lengths of the three sub-spans are $l_1 = 0.6/a_0$, $l_2 = 0.4/a_0$, and $l_3 = 0.5/a_0$ with $a_0 = 0.0955$ m. The thickness of the rotor disk is assumed to be much smaller than the span length and the diameter of the disk is $4a_0$. The spring constants are $k_t = 0.3814$ and $k_r = 113$. It is determined that $A(\omega) > 0$ over the entire frequency range and that the non-zero cutoff frequency $\omega_c \cong 4.1546$. Thus, in Fig. 7, $B(\omega) < 0$ (since $\omega < \omega_c$) and the wave motion is governed by the solution of Case II. The reflection and transmission matrices $\mathbf{r}_{II}$ and $\mathbf{t}_{II}$ are used at the boundaries and at each station. Note that $\mathbf{r}_{II}$ for the simply supported boundaries is

$$\mathbf{r}_{II} = \begin{bmatrix} -1 & 0 \\ 0 & -1 \end{bmatrix}.$$

In Fig. 7, it is seen that small frequency increments $\Delta\omega$ may be required to find the natural

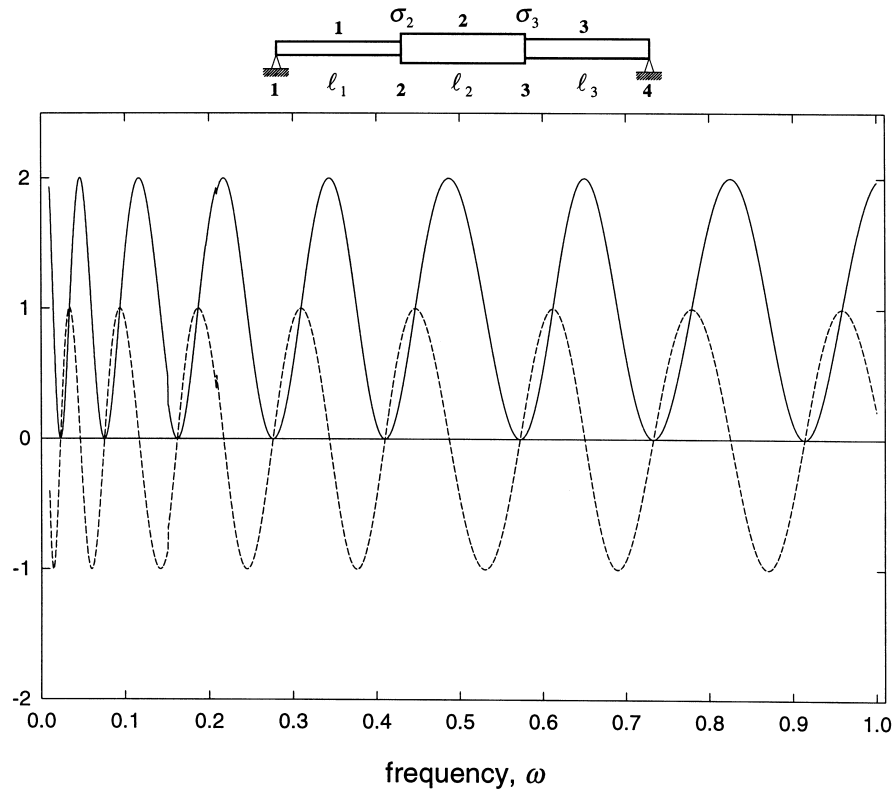

Fig. 8. Plot of $C(\omega)$ as a function of frequency, $\alpha = 0.3378$, $\beta = 0.05$, $\varepsilon = 0.002$, $\sigma_2 = (a_1/a_2) = 0.8$, $\sigma_3 = (a_2/a_3) = 1.2$, $l_1 = l_2 = l_3 = 0.5/a_0$, $a_3 = a_0 = 0.0955$ m; Re $[C(\omega)]$ (—), Im $[C(\omega)]$ (- - -).

frequencies. The drastic variations of $C(\omega)$ are caused by some of the eigenvalues of the sub-spans being very close to the eigenvalues of the shaft system.

The third example is a rotating shaft with three spans of equal length but different diameters. A tensile load is applied to the shaft. A schematic of the system is depicted on the top of Fig. 8. The total length of the shaft is 1.5 m. The diameters of the sub-spans are $d_1 = 0.96a_0$, $d_2 = 1.2a_0$, and $d_3 = a_0 = 0.0955$ m. Figure 9 outlines a computational flow chart for $C(\omega)$ of this problem. Note that this computer algorithm can be systematically coded and generalized for the solutions of rotating shafts with multiple sub-spans and discontinuities. In this example, because of the geometric discontinuities in the cross-section, the forms of the wave solution change from one sub-span to another and as the frequency is varied. This is manifested in the 'kinks' of Fig. 8. The wave solutions of the sub-spans 1, 2, and 3 change from Case IV to Case II at $\omega \cong 0.15$, $\omega \cong 0.195$, and $\omega \cong 0.21$, respectively.

6. Summary and conclusions

In this paper, a systematic approach based on wave propagations is presented to study the free vibration of a rotating, multi-span Timoshenko shaft subjected to axial forces. The complicating

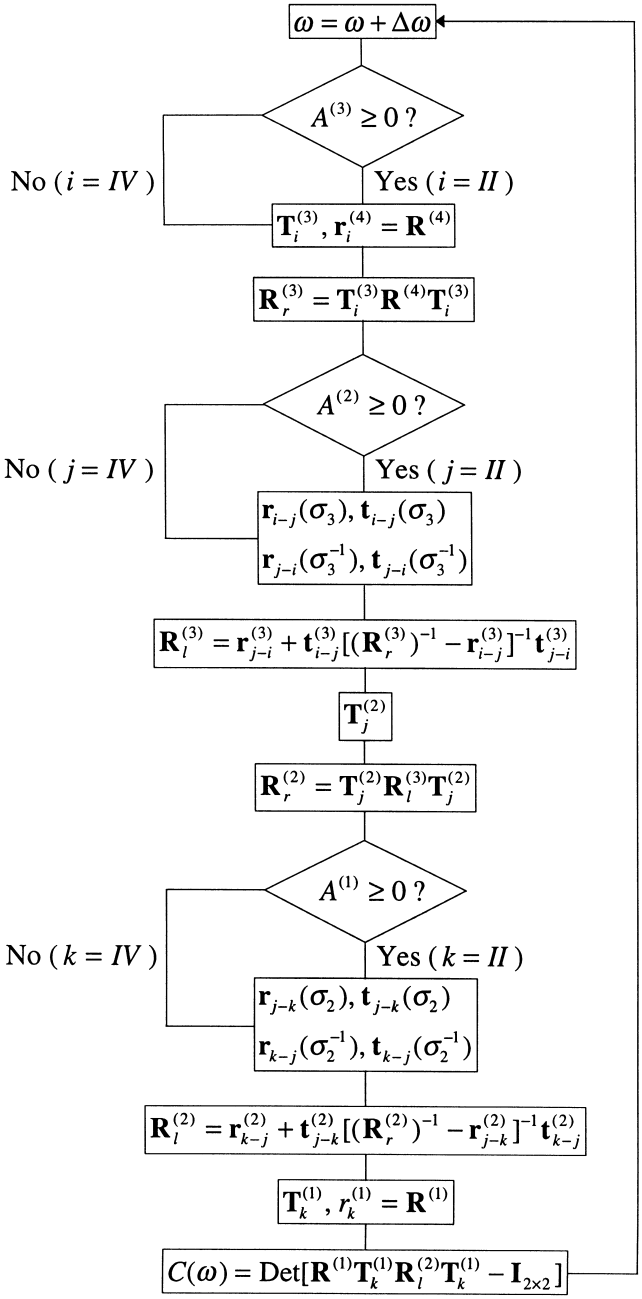

Fig. 9. A numerical algorithm for computing $C(\omega)$ for the system of example 3. Superscripts denote station numbers (or span numbers for A and $\mathbf{T}$). Subscripts i, j, and k denote the type of wave motions (Case I, II, or IV). Note that $B > 0$ for the given range of frequencies.

effects of axial force, rotation speed and shear on the wave motions are treated in a unified manner by examining the characteristics of the wavenumbers. Including the effects of attenuating wave components, the wave motions at the discontinuities and in the sub-spans are described exactly by the wave reflection and transmission matrices and the field transfer matrices expressed in wave forms, respectively. By applying the wave-train closure principle, characteristic equations of complex rotating shaft systems can be obtained in a straightforward manner. The proposed wave approach results in recursive computational algorithms and the numerical effort does not involve computations of matrices with large orders which may occur in the general method of transfer matrix. These advantages render the wave methodology suitable for computer coding.

Acknowledgements

The authors gratefully acknowledge the support of the National Science Foundation and the Institute for Manufacturing Research of Wayne State University for this research work.

References

Argento, A., Scott, R.A., 1995. Elastic wave propagation in a Timoshenko beam spinning about its longitudinal axis. Wave Motion 21, 67–74.

Choi, S.H., Pierre, C., Ulsoy, A.G., 1992. Consistent modeling of rotating Timoshenko shafts subject to axial loads. ASME Journal of Vibration and Acoustics 114, 249–259.

Cremer, L., Heckl, M., Ungar, E.E., 1973. Structure-Borne Sound. Springer-Verlag, Berlin.

Fahy, F., 1985. Sound and Structural Vibration. Academic Press.

Graff, K.F., 1975. Wave Motion in Elastic Solids. Ohio State University Press.

Han, R.P.S., Zu, J.W.Z., 1992. Modal analysis of rotating shafts: a body-fixed axis formulation approach. Journal of Sound and Vibration 156, 1–16.

Huang, T.C., 1961. The effect of rotary inertia and of shear deformation on the frequency and normal mode equations of uniform beams with simple end conditions. ASME Journal of Applied Mechanics 28, 579–584.

Holzer, H., 1921. Die Berechnung der Drehschwingungen. Springer-Verlag. Berlin.

Kang, B., Tan, C.A., 1998. Elastic wave motions in an axially strained, infinitely long rotating Timoshenko shaft. Journal of Sound and Vibration, in press.

Katz, R., Lee, C.W., Ulsoy, A.G., Scott, R.A., 1988. The dynamic response of a rotating shaft subject to a moving load. Journal of Sound and Vibration 122, 131–148.

Lee, A.-C., Kang, Y., Liu, S.-L., 1991. A modified transfer matrix method for linear rotor-bearing systems. ASME Journal of Applied Mechanics 58, 776–783.

Lee, C.W., Katz, R., Ulsoy, A.G., Scott, R.A., 1988. Modal analysis of a distributed parameter rotating shaft. Journal of Sound and Vibration 122, 119–130.

Lin, Y.K., Donaldson, B.K., 1969. A brief survey of transfer matrix techniques with special reference to the analysis of aircraft panels. Journal of Sound and Vibration 10, 103–143.

Mace, B.R., 1984. Wave reflection and transmission in beams. Journal of Sound and Vibration 97, 237–246.

Mead, D.J., 1994. Waves and modes in finite beams: application of the phase-closure principle. Journal of Sound and Vibration 171, 695–702.

Myklestad, N.O., 1944. A new method of calculating natural modes of uncoupled bending vibration of airplane wings and other types of beams. Journal of Aeronautical Sciences 11, 153–162.

Pestel, E.C., Leckie, F.A., 1963. Matrix Methods in Elastomechanics. McGraw-Hill, New York.

Popplewell, N., Chang, D., 1997. Free vibrations of a stepped, spinning Timoshenko beam. Journal of Sound and Vibration 203, 717–722.

Subrahmanyam, K.B., Garg, A.K., 1997. Uncoupled flexural vibrations of straight beams with all possible boundary conditions treated by a transfer matrix method. Journal of Sound and Vibration 204, 397–419.

Tan, C.A., Kang, B., 1998. Wave reflection and transmission in an axially strained, rotating Timoshenko shaft. Journal of Sound and Vibration, in press.

Tan, C.A., Kuang, W., 1995. Vibration of a rotating discontinuous shaft by the distributed transfer function method. Journal of Sound and Vibration 183, 451–474.

Tsai, T.C., Wang, Y.Z., 1996. Vibration analysis and diagnosis of a cracked shaft. Journal of Sound and Vibration 192, 607–620.

Yang, B., Fang, H., 1994. Transfer function formulation of non-uniformity distributed parameter systems. ASME Journal of Vibration and Acoustics 116, 426–432.

Yong, Y., 1991. Vibration of Euler–Bernoulli beams with arbitrary boundaries and intermediate constraints. Machinery Dynamics and Element Vibrations ASME DE-Vol. 36, pp. 119–128.

Zu, J.W.Z., Han, R.P.S., 1992. Natural frequencies and normal modes of a spinning Timoshenko beam with general boundary conditions. ASME Journal of Applied Mechanics 59, 197–204.